Cauchy pressure and the generalized bonding model for nonmagnetic bcc transition metals

Mark E. Eberhart[1,*] and Travis E. Jones[1,2]

[1]*Molecular Theory Group, Colorado School of Mines, Golden, Colorado 80401*

[2]*School of Physics, The University of Sydney, Sydney, New South Wales 2006, Australia*

(Received 20 May 2012; revised manuscript received 7 August 2012; published 5 October 2012)

The chemical bond as a physical linkage between atoms has proven to be an immensely powerful heuristic device, providing insight into the general relationships between the structure and properties of molecules and solids. Unfortunately, the bond concept is incomplete and fails to explain more subtle aspects of molecular and materials behavior. A rich set of examples is provided by attempts to identify the structural origins of nonzero Cauchy pressures, a quantity that has been said to reflect the nature of the bonding at the atomic level. We show that these deviations are easily explained by extending the concept of a bond from a linkage between atoms to a set of linkages between charge density critical points (maxima, minima, and saddle points). Further, we show that these links possess an identifiable structure with measurable characteristics. For the nonmagnetic bcc transition metals, we are able to write the Cauchy pressure as a function of these characteristic measures. Significantly, the model should be generalizable to other structures and will provide insight into the relationships between the charge density and elastic response.

DOI: 10.1103/PhysRevB.86.134106 PACS number(s): 64.70.K−

I. INTRODUCTION

We report our efforts to describe the full range of atomic interactions with a general bonding model (GBM) that retains the elegance of a bond as a spring like link. The GBM is motivated by resent extensions to the quantum theory of atoms in molecules (QTAIM),[1–4] which have demonstrated that the charge density my be partitioned into volumes—irreducible bundles—diffeomorphic to tetrahedra that are also proper open systems within the QTAIM formalism. As tetrahedra, irreducible bundles (IBs) are also simplices and, therefore, can be glued together both in a topological sense and as open systems to produce simplical complexes whose realization is the charge density of any molecule or solid. The underlying graph, or 1-skeleton, of the resulting complex is related to the common molecular graph representing bonds between atoms as links. However, a molecule's underlying graph provides more information than does the molecular graph. And, we believe, provides quantitative insight into the origin of a molecule or solid's elastic properties.

The relative magnitudes of a solid's elastic moduli are indicative of mechanical and phase behavior.[5–7] Despite their importance and the fact that first-principles methods can be used to calculate their values, there is no simple model that allows one to explain, for example, why the shear modulus of Ir is greater than that of Pt. In this work, a model that accounts for the variation of the Cauchy pressure across the topologically simple nonmagnetic bcc transition metals is introduced.

A. Topological structure of the charge density

In building the GBM we are exploiting Bader's quantum theory of atoms in molecules (QTAIM),[1] which, as a topological theory, is ideally suited to describe linkages between atoms. In its original formulation, QTAIM was concerned with the topological connections between volumes bounded by a specific set of surfaces on which the gradient of the charge density vanishes at every point. Such surfaces are referred to as zero flux surfaces (ZFSs). By virtue of being bounded by ZFSs, these volumes are proper open systems characterized by properties that are in principle measurable.[1,8–11] Though there are infinitely many such volumes,[12,13] the initial formulation of QTAIM involved only those where the bounding ZFSs did not intersect an atomic nucleus. These distinct volumes, called Bader atoms or sometimes atomic basins, partition the charge density of a molecule or solid into space filling regions each of which encloses a single nucleon—hence the name, "atom."

In turn, Bader atoms can be connected variously as reflected by the charge density's rank three critical points (CPs). These are the places where the charge density, a three-dimensional scalar field, achieves extreme values in all directions. As with all 3D scalar fields, the charge density possesses at most four kinds of CP: local minima, local maxima, and two types of saddle points. These CPs are denoted by an index, which is the number of principal positive curvatures minus the number of principal negative curvatures. For example, at a minimum, the curvature in all three orthogonal directions is positive; therefore it is called a (3, +3) CP. The first number is simply the number of dimensions of the space and the second is the net number of positive curvatures. A maximum is denoted by (3, −3), because all three curvatures are negative. A saddle point with two of the three curvatures negative is denoted (3, −1), while the other saddle point is a (3, +1) CP.

The charge density at the atomic nucleus is always a maximum, i.e., a (3, −3) CP, hence it is also called a nuclear CP. The other CPs, which must be present in a molecular system, sit on the ZFSs bounding the Bader atoms and mediate their connectivity.[1,8,14,15] The simplest topological connection results from a shared (3, −1) CP between two Bader atoms, and is indicative of a charge density ridge originating at the (3,−1) CP and terminating at the nuclear CPs. In essence, this charge density ridge possesses the topological properties imagined for the chemical bond, which motivated studies showing the presence of such a ridge between atoms that conventional wisdom assumed to be bound. Accordingly, this ridge is descriptively referred to as a bond path and the accompanying (3, −1) CP as a bond CP. Other types of CPs have been correlated with other features of molecular connectivity. A

 ©2012 American Physical Society

(3, +1) CP is required at the center of ring structures (rings of bond paths). Accordingly, it is designated a ring CP. Cage structures must enclose a single (3, +3) CP and are given the name cage CPs.

Though only recently noted,[2–4,16,17] CPs, bond paths, and the ZFSs of Bader atoms are elements drawn from the larger set of extremal points, lines, and surfaces. These extremals are generically referred to as ridges and valleys. In 2D, a ridge is a familiar topographic feature, the path (gradient path) connecting mountain passes to neighboring peaks, for example. There is only one such gradient path; and it is a path of locally least steep ascent terminating at the local maximum. Consequently, it is an extremum with respect to all neighboring paths. Similarly, a valley is an extreme gradient path connecting a saddle point to a local minimum. Because valleys and ridges differ only by the sign of the curvatures along the path, both are often referred to as "ridges." In 3D fields (the electron charge density), ridges are the points, gradient paths, and zero flux surfaces that are extreme with respect to all neighboring points, gradient paths, and zero flux surfaces, respectively. They are denoted by an index, $n - d$, where n is the dimensionality of the space and d is the number of principal directions in which the charge density is extremal.[18] Thus a 0-ridge is nothing more than one of the four types of critical points. A 1-ridge is an extremal gradient path, of which the bond path is an example, and a 2-ridge is an extremal gradient surface, of which the ZFSs bounding Bader atoms are examples.

For an extended systems—infinite solids—there will always be four kinds of charge density CPs (0-ridges), six kinds of 1-ridges, and four kinds of 2-ridges. The 1-ridges pairwise connect the four kinds of critical points and the 2-ridges are surfaces containing three distinct CPs. The ridge structure forms a set of space filling volumes diffeomorphic to a tetrahedron and called irreducible bundles. Coincident with the four vertices of each irreducible bundle (IB) is a nuclear, bond, ring and cage CP, respectively. The six edges of the tetrahedron are 1-ridges, and the four faces are 2-ridges, Fig. 1.

As tetrahedra, the IBs are simplices, and by virtue of the fact that they are also proper open systems bound by ZFSs, they are the most basic unit of charge density retaining local topology. As such, IBs may be glued together to form a simplical complex that is isomorphic to the charge density of any molecular system. By way of illustration, Fig. 2 shows the symmetry unique IB that can be joined to produce the bcc Wigner Seitz cell, which can then be joined to form a larger simplical complex—the extended bcc crystal.

From a molecule or solid's simplical complex one can construct subcomplexes, called d-skeletons, which recover the charge density at various topological levels. In particular, the 0-skeleton of the simplical complex is the set of all of its CPs. Its 1-skeleton consists of all 1-ridges and is called the underlying graph of the complex. The 2-skeleton is the set of all 2-ridges, and the 3-skeleton is the full simplical complex. We are particularly interested in a molecule or solid's underlying graph, which as a subset contains the molecular graph common to depictions of molecules. However, the molecular graph depicts only bond paths, i.e., the connections between atoms, while the underlying graph (1-skeleton) depicts the full set of 1-ridges and their points of intersection, the CPs of the charge

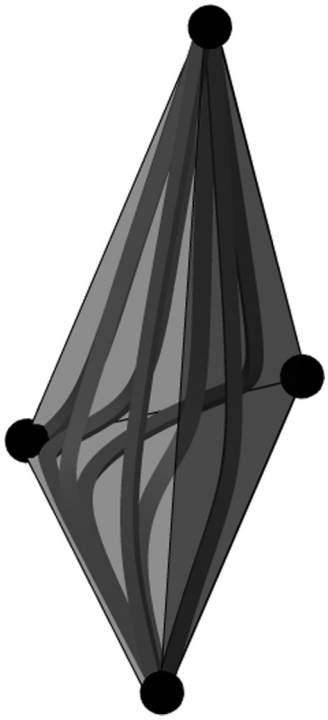

FIG. 1. An irreducible bundle of fcc Cu, showing the Cu nuclear CP (top), the ring point (middle left), the bond point (middle right), and the cage point (bottom). The dark rods are gradient paths originating at the cage CP and terminating at the atom CP. The gradient paths in the IB are confined to the shaded tetrahedral volume and are characterized by both curvature and torsion. The faces of this tetrahedron are 2-ridges each containing three CPs.

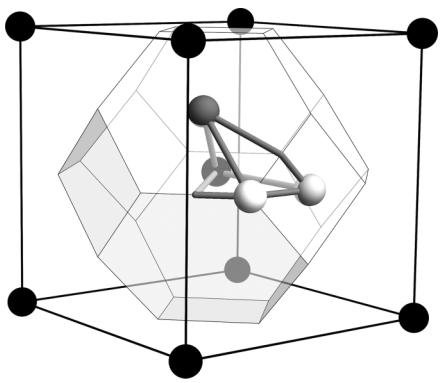

FIG. 2. The conventional cubic bcc unit cell, the surface of the Bader atom (Wigner-Seitz cell) is the shaded truncated octahedron. A nuclear CP is located at its center. Ring CPs are located at every vertex, bond CPs in the center of every hexagonal face, and cage CPs in the center of each square face, giving a total of 39 critical points in or on the surface of the Bader atom. The four symmetry unique CPs are designated with spheres (black for nuclear, dark gray for bond, white for ring, and light gray for cage) and the symmetry unique paths of the ridges and valleys connecting these CPs, the edges of the irreducible bundle, are shown as gray tubes. Within the GBM there are 134 such connections that are treated as straight springs.

density. Together these structures capture the full topology of the atomic connections.

B. Geometric structure of the charge density

The geometry of the charge density can be characterized at various levels through the specific values of the extremal features of the n-skeletons. As an example, Ayers and Jenkins[19,20] have proposed a dynamical theory of electronic response using a subset of the information available from the charge density's underlying graph. They treated bond critical points as pseudoparticles that, when moved, drag the nuclear cp along by virtue of their connections through bond paths (1-ridges). The validity of this assumption derives from the observation that the eigenvectors of the Hessian of the charge density $[\rho(\vec{r})]$, the second derivative matrix, at a CP are good approximations to the eigenvectors of the quantum stress tensor—the quantum operator that mediates the electronic response to deformation. The effectiveness of this perspective was substantiated by predicting the direction of structural change during the pressure-induced phase transition in ice[19] and formation of new bond paths during chemical reactions.[20]

With this background, it is not a great leap to evoke the underlying graph as the GBM's representation for a molecule and consider all critical points as pseudo-particles joined along 1-ridges by Hookean springs characterized by their stiffness alone. Motivated by Ayers and Jenkins,[19,20] we begin by making a "local" approximation and conjecture that the spring constants can be approximated by functionals of the charge density in the neighborhood of the corresponding 1-ridge's end point, i.e., at the CPs. In particular, we expect that the charge density and its curvatures at these points will most influence the value of the spring constants.

II. METHODS

All calculations were performed using the Vienna *ab initio* simulation package (VASP) version 4.6[21,22] with the standard PAW potentials[23] and the Perdew-Burke-Ernzenhof generalized gradient corrections (PBE).[24] To ensure there was no dependence on the exchange and correlation potential a second set of calculations were performed with the Perdew-Wang (PW91) generalized gradient corrections[25] and the Vosko-Wilk-Nusair interpolation of the correlation part of the exchange-correlation functional.[26] Because the geometric and topological properties were not sensitive to this choice we only report the results of the PBE calculations, which were analyzed using TECPLOT.[27]

III. MODEL

We start with the nonmagnetic bcc transition metals because, of the common crystal structures, only the bcc structure possesses the simplest possible topology, with one symmetry unique nuclear, bond, ring and cage CP and hence (the minimum) six different 1-ridges. These 1-ridges are shown in Fig. 2. Two of these are bent—the bond CP to cage CP and the nuclear CP to ring CP—a fact that is transparent to the GBM. We adopt the notation k_{cp1cp2} to denote the spring constant of the link joining $cp1$ to $cp2$, where a cp can be n, b, r, or c for nuclear, bond, ring, and cage, respectively. Thus k_{br} corresponds to the spring constant of the bond to ring CP connection.

TABLE I. bcc elastic constants (10^{10} Pa).

	Mo	Nb	Ta	V	W
C_{11}	45.00	25.27	28.63	23.24	53.26
C_{12}	17.29	13.32	15.82	11.94	20.50
C_{44}	12.50	3.10	8.74	4.60	16.31
$C_{12}-C_{44}$	4.79	10.22	7.08	7.34	4.18

As with all cubic crystals, the elastic response of this entire set of springs is tied to three independent elastic constants: C_{11}, C_{12}, and C_{44} (see Table I), each of which can be expressed as a linear combination of the six symmetry unique spring constants. The procedure through which this relationship is derived begins by distorting the entire system with a homogenous strain, the corresponding displacement of the CPs is determined along with the extension of the connecting springs and hence the elastic energy of the system. The energy terms quadratic in the strain are then mapped onto the single crystal elastic constants (see for example, Ref. 28). This procedure gives

$$\begin{aligned} C_{11} &= V_a^{-\frac{1}{3}}(0.67k_{nb} + 6.80k_{nr} + 2k_{nc} + 13.96k_{br} \\ &\quad + 7.31k_{bc} + 14.56k_{rc}), \\ C_{12} &= V_a^{-\frac{1}{3}}(0.67k_{nb} + 1.60k_{nr} + 0k_{nc} + 8.76k_{br} \\ &\quad + 3.31k_{bc} + 1.69k_{rc}), \\ C_{44} &= V_a^{-\frac{1}{3}}(0.67k_{nb} + 1.60k_{nr} + 0k_{nc} + 5.67k_{br} \\ &\quad + 1k_{bc} + 0.80k_{rc}), \end{aligned}$$

where V_a is the atomic volume.

Note that the quantity $C_{12}-C_{44}$, called the Cauchy pressure, is a function of only three spring constants:[6]

$$C_{12} - C_{44} = V_a^{-\frac{1}{3}}(3.10k_{br} + 2.31k_{bc} + 0.89k_{rc}), \qquad (1)$$

where all terms related to connections with the nuclear CP have dropped out.

Systems where the Cauchy pressure is zero are indicative of atoms interacting through a central force potential, which includes simple spring like connections and accounts for the fact that connections with the nuclear CP have dropped out. Positive deviations reflect "metallic bonding," which necessitates corrections involving "many-body interactions that result when an atom interacts with the electron gas of its neighbors." Negative Cauchy pressures derive from "covalent bonding character" and require angular corrections.[29]

The simplified nature of Eq. (1) makes it somewhat easier to guess at the relationship between the structure of the charge density at two connected CPs and the spring constant of that link. Additional insight is gained by considering the stiffness tensor from a DFT perspective,[30,31] where the energy of an atomic system is expressed as a function of nuclear position $q(R_i)$ and a functional of the charge density; $E = E[q(R_i), \rho(\vec{r}, R_i)]$, where R_i represents the coordinates

of the ith atom. The macroscopic elastic properties originate through the variation of this energy accompanying collective nuclear distortions from the ground state configuration. These distortions can be fully parameterized within a six dimensional vector space of strains ϵ_{ij} and we denote these nuclear coordinates as Q_{ij}, where the subscripts have the same sense as in the strain tensor. The elastic energy is now a function of the nuclear strain coordinate and a functional of the density $E = E[q(Q_{ij}), \rho(\vec{r}, Q_{ij})]$. The stress tensor $\sigma_{\mu\nu}$ is given by the variational derivative of the system energy with respect to Q_{ij}, i.e.,

$$\sigma_{ij} = \frac{\partial E}{\partial Q_{ij}} + \int dV \frac{\partial \rho(\vec{r})}{\partial Q_{ij}} \frac{\delta E}{\delta \rho(\vec{r})}. \tag{2}$$

Since the electrons are allowed to relax to positions that minimize the total energy, $\frac{\delta E}{\delta \rho(\vec{r})} = 0$. Hence $\sigma_{ij} = \frac{\partial E}{\partial Q_{ij}}$. This is simply a generalization of the Hellmann-Feynman theorem.

Though the stress at a nucleus is given purely by electrostatics involving the charge density; the change in this stress with strain—the elastic stiffness—requires that one take the variational derivative of Eq. (4) with respect to the nuclear strain coordinate, giving

$$C_{ijkl} = \frac{\partial^2 E}{\partial Q_{ij} \partial Q_{kl}} + \iint dV dV' \frac{\partial \rho(\vec{r}')}{\partial Q_{ij}} \frac{\partial \rho(\vec{r})}{\partial Q_{kl}} \frac{\delta^2 E}{\delta \rho(\vec{r}) \delta \rho(\vec{r}')}, \tag{3}$$

where C is the fourth-rank stiffness tensor of elasticity theory.

The origins of the stiffness can be seen to be due to two terms. The first of these is the stiffness experienced by a collective motion of the nuclei through a fixed charge distribution. The second is the result of variations in the charge density—the charge redistribution. Of the three terms in the integrand, the first two, $\frac{\partial \rho(\vec{r}')}{\partial Q_{ij}}$ and $\frac{\partial \rho(\vec{r})}{\partial Q_{kl}}$ gives the change in charge density induced by the strain at the points r' and r, while the quantity $\frac{\delta^2 E}{\delta \rho(r) \delta \rho(r')}$ measures of the variation of the energy due to the correlated change in charge density at two points r and r'. Functionally, when r and r' are separated by distances on the order of atomic units this term goes as $\frac{1}{|\vec{r} - \vec{r}'|}$, i.e., inversely as the distance between the two differential volume elements. In most systems, at small distances this term approaches zero as r approaches r'. The integrand is interpreted as measuring the coupling of charge redistribution between two volume elements.

We make a conceptual simplification to the integral of Eq. (3) by adopting a reasonable form for $\frac{\delta^2 E}{\delta \rho(r) \delta \rho(r')}$. This form associates a volume V_{cp} with each critical point such that every point r is contained in only one volume and defines as connected CPs joined by a 1-ridge, hence, only CPs within the same irreducible bundle may be in connected. With these concepts and definitions, we assume: (1) for r and r' in unconnected CP volumes, i.e., far apart, $\frac{\delta^2 E}{\delta \rho(r) \delta \rho(r')} = 0$; (2) for r and r' located in the same CP volume, i.e., close together, $\frac{\delta^2 E}{\delta \rho(r) \delta \rho(r')} = 0$; and (3) for r and r' located in connected volumes, $\frac{\delta^2 E}{\delta \rho(r) \delta \rho(r')} = C_{cp1,cp2} > 0$, where $C_{cp1,cp2}$ is a constant that depends on the connected volumes.

With these assumptions, the integral of Eq. (3) becomes

$$\begin{aligned} &\iint dV dV' \frac{\partial \rho(\vec{r}')}{\partial Q_{ij}} \frac{\partial \rho(\vec{r})}{\partial Q_{kl}} \frac{\delta^2 E}{\delta \rho(\vec{r}) \delta \rho(\vec{r}')} \\ &= \sum_{cp1} \sum_{cp2 \neq cp1} C_{cp1,cp2} \left[\int dV_{cp1} \frac{\partial \rho(\vec{r})}{\partial Q_{ij}} \int dV_{cp2} \frac{\partial \rho(\vec{r})}{\partial Q_{kl}} \right. \\ &\quad \left. + \int dV_{cp1} \frac{\partial \rho(\vec{r})}{\partial Q_{kl}} \int dV_{cp2} \frac{\partial \rho(\vec{r})}{\partial Q_{ij}} \right]. \end{aligned} \tag{4}$$

In this form, the component of the stiffness tensor given by Eq. (4) quantify the coupling of charge redistribution in different critical point volumes. A classical analogy is provided by elastic elements subject to load; these elements couple through their load induced change in shape. The stiffer the element, the smaller the shape change. In a comparable way, the intercritical point spring constants, as in Eq. (1), relate the charge redistribution to the change in shape of these CP volume.

The shape of the charge density about a CP is well approximated by its Hessian $[\mathcal{H}_{ij} \rho(\vec{r}) = \frac{\partial^2 \rho(\vec{r})}{\partial x_i \partial x_j}]$, which has the same transformation properties as the coefficients of a quadratic polynomial referred to as the representation quadric.[32,33] When expressed in a diagonal basis, the representation quadrics is given by the equation

$$\rho_{11} x_1^2 + \rho_{22} x_2^2 + \rho_{33} x_3^2 = 1,$$

where x_1, x_2, and x_3 are the orthogonal directions in which the curvature of the charge density achieves its extreme values and ρ_{11}, ρ_{22}, and ρ_{33} are the curvatures of the charge density in these directions.

At a cage CP, where all principal curvatures are positive, the representation quadric is an ellipsoid. A ring CP, having one negative principal curvature, is represented by a hyperboloid of one sheet; and the representation quadric of a bond CP (two negative principal curvatures) is a hyperboloid of two sheets. We will also consider the asymptotic elliptic cones associated with the hyperboloids of the bond and ring CPs (the surfaces given by the equation $\rho_{11} x_1^2 + \rho_{22} x_2^2 + \rho_{33} x_3^2 = 0$). As the charge density at a nuclear CP is a cusp, its curvatures and representation quadric are not well defined.

IV. RESULTS

Consider now the specific case of the nonmagnetic bcc transition metals. Because the eigenvectors of the Hessians for different bcc metals are identical, and the eigenvalues are symmetry constrained, only nine independent terms representing the shape of the charge density about bcc CPs need be determined. These are the charge density at the cage, ring, and bond points, and at each of these points two independent charge density principal curvatures derived from a degenerate pair and a singlet. These values are given in Table II.

Figure 3 provides a particularly useful visual presentation of this information by plotting the representation quadric of the cage CP and asymptotic cones to the representation quadrics of the bond and ring CPs. For the bcc structure, these are right circular cones and are fully described by a single angle. In our notation, the apex angle is denoted by $2\phi_{\text{cp}}$ and the exterior angle by $2\theta_{\text{cp}}$ ($\phi + \theta = 90^\circ$). These angles are given by ratios

TABLE II. Values of the nine independent shape descriptors for the bcc metals: $\rho_{\rm cp}$ gives the value of the charge density at a cage (c), ring (r), or bond (b) point in units of electrons per Å^3, $^{\rm cp}\rho_{11}$ gives the nondegenerate principal value of the curvatures at the critical point specified by the superscript and $^{\rm cp}\rho_{22}$ is the value of its degenerate principal curvature in units of electrons per Å^5.

	ρ_c	ρ_r	ρ_b	$^c\rho_{11}$	$^c\rho_{22}$	$^r\rho_{11}$	$^r\rho_{22}$	$^b\rho_{11}$	$^b\rho_{22}$
Mo	0.243	0.258	0.370	0.509	0.120	−0.113	0.209	3.477	−0.713
Nb	0.203	0.215	0.282	0.327	0.094	−0.087	0.094	2.389	−0.394
Ta	0.223	0.235	0.301	0.255	0.077	−0.087	0.156	1.938	−0.343
V	0.216	0.225	0.253	0.139	0.086	−0.068	0.069	0.507	−0.177
W	0.265	0.286	0.411	0.532	0.170	−0.162	0.231	3.354	−0.783

of the principal curvatures of the Hessian. The values of θ_b are approximately: Mo = 24°, Nb = 22°, Ta = 23°, V = 30.5°, and W = 26°. For the ring CP, the θ_r are approximately: Mo = 36°, Nb = 44°, Ta = 36.5°, V = 45°, and W = 40°. Finally, there is an equivalent set of angles for the cage CP that are related to the eccentricity of the ellipsoid and are: Mo = 64°, Nb = 62°, Ta = 62°, V = 52°, and W = 60.5°

The asymptotic cones mark boundaries of a sort. Close to the CP, these cones are isosurfaces of the charge density. The isosurfaces exterior to the cone are curved oppositely from those interior to the cone. As a result, the gradient paths turn as they cross the cone, transitioning from divergent to convergent paths. To illustrate the point, Fig. 4 shows a series of gradient paths in the 2-ridge containing the nuclear, bond, and ring CPs. Note that the gradient paths coming from the nuclear CP are diverging, while after crossing the cone they are converging. The same is true for a general gradient path. Ostensibly, these cones act to "divert" and "concentrate" or "focus" gradient paths. Further concentration occurs as the gradient paths cross the asymptotic cone of the ring CP.

The family of gradient paths passing through the asymptotic cones of the bond and ring CPs will fill volumes of the type introduced in Eq. (4). The key here is that these volumes are distinct (by virtue of the their gradient field), should reflect the form of charge redistribution, and can be approximated by just four parameters—the angles characteristic of the representation quadrics, and the charge densities at the connected critical points. Previously, Eberhart[31] suggested that the strain induced mobility of electrons about a bond CP goes as $\rho_b\theta_b$ or equivalently as $\rho_b \tan(\theta_b)$. Accordingly, we propose as an ansatz that the total strain induced electron mobility between the ring and bond, for example, goes as $\rho_r \tan(\theta_r)\, \rho_b \tan(\theta_b)$ and the spring constant will be proportional to the reciprocal of this quantity, less a comparatively small constant (the meaning of which will become clear), giving

$$k_{rb} \propto \frac{1}{\rho_r \tan(\theta_r)\rho_b \tan(\theta_b)} - \kappa_{rb} = \frac{\tan(\phi_r)}{\rho_r \rho_b \tan(\theta_b)} - \kappa_{rb}.$$

For conceptual reasons, we write this expression in a nearly identical form as

$$k_{rb} \propto \frac{\phi_r}{\rho_r \rho_b \theta_b} - \kappa_{rb}. \tag{5}$$

Similarly, the other spring constants are given by

$$k_{cr} \propto \frac{\phi_c}{\rho_c \rho_r \phi_r} - \kappa_{cr}, \tag{6}$$

$$k_{cb} \propto \frac{\theta_c}{\rho_c \rho_b \theta_b} - \kappa_{cb}. \tag{7}$$

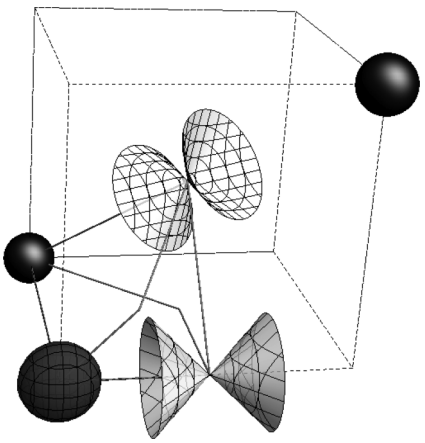

FIG. 3. A representation of the the charge density around the CPs of bcc tungsten for one irreducible bundle. The two near neighbor bound nuclei are shown as spheres located in the lower back left-hand corner and upper front right-hand corner. The 1-ridges coincident with the edges of the irreducible bundle are shown as lines. A scaled representation quadric for the cage CP is located in the lower left-hand corner. Also shown are the asymptotic cones to the representation quadrics ($\rho_{11}x_1^2 + \rho_{22}x_2^2 + \rho_{33}x_3^2 = 0$) of the bond CP (center) and ring CP (center bottom).

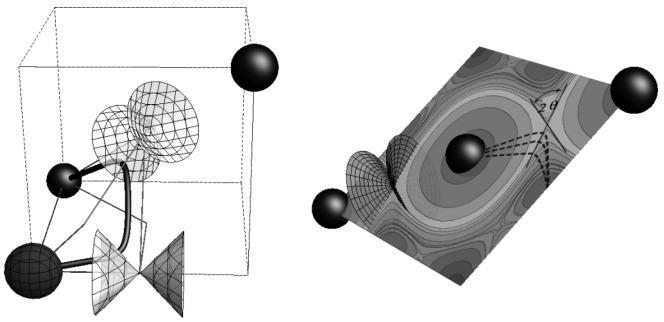

FIG. 4. Gradient paths crossing the asymptotic cone of the bond CP in tungsten. (Right) Contour diagram of the computed charge density of W in a plane containing a nuclear, bond and ring CP, a (211) plane. The gradient paths are shown as dashed lines. The full asymptotic cone is shown in the lower left-hand corner while its trace in the plane is shown in the upper righthand corner. The angle θ is related to the relative magnitude of the principal curvatures of the Hessian of the charge density, specifically, $\tan(\theta) = \sqrt{\frac{\rho_{22}}{\rho_{11}}}$. (Left) The full trajectory of a general gradient path. Note the concentration of path curvature and torsion near the asymptotic cones of the ring and bond CP.

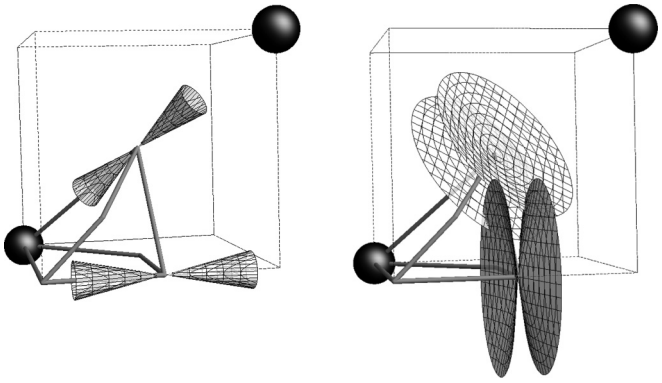

FIG. 5. Two extreme ring to bond interactions. (Left) A ring and bond connected by gradient paths confined to a comparatively large cross section, hence possessing a smaller value of k_{br} than the case represented (right) where the ring and bond CP interact through a smaller cross section.

According to these relationships, large values of k_{cp1cp2} result when CPs interact through a small cross section, Fig. 5, and small (possibly negative) values result from large interaction cross sections.

To test this conjecture, the parameters tabulated in Table II have been used in conjunction with Eqs. (1) and (5)–(7) to predict the relative values of the Cauchy pressure for each of the bcc transition metals and then plotted against the measured values of the same quantity, Fig. 6. For such a simple model, the correlation is quite good, with $R^2 = 0.975$ for the best linear fit.

It is important to note that in settling on the form of Eqs. (5)–(7), we investigated many alternative expressions, first using principal component analysis to isolate the parameters most important in determining the intercritical point spring constants and then through trial and error exploration of hundreds of functional forms involving these parameters. Equations (5)–(7), and those conceptually similar, were demonstrably better than all others. Happily they were also consistent, though not identical, with the notions presented in earlier papers,[31] where it was argued that $\tan\theta_b$ provided a measure of the distance to "bond breaking." In other words, $\tan\theta_b$ must vanish if the bond

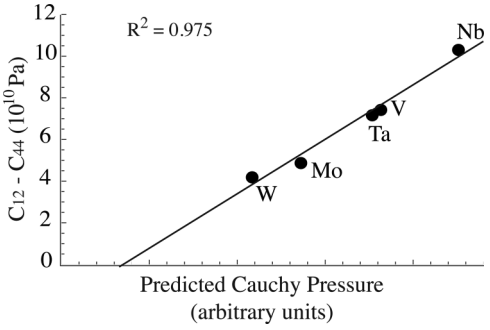

FIG. 6. Predicted vs measured values of the Cauchy pressure for five bcc metals. The best linear fit gives an R^2 of 0.975. The intercept of this line with the horizontal axis allows one to estimate an average κ.

TABLE III. The effective intercritical point spring constants in units of 10^{10} Pa.

Connection type	Mo	Nb	Ta	V	W
Ring to bond	0.932	2.309	1.486	1.487	0.834
Cage to bond	0.590	1.257	0.925	0.780	0.501
Cage to ring	0.797	1.208	1.087	1.043	0.692

point is to vanish. Hence the quantity $\rho_b \tan\theta_b$ is proportional to the charge that must be moved to break a bond.

For the current application, the issue is the charge that must be moved to make the Cauchy pressure vanish. The Cauchy pressure goes to zero when the charge density takes on a shape resulting from the overlap of spherically symmetric densities. This "reference state," though built from overlapping spherical charge densities, will likely continue to be characterized by a bcc topology with values for all the shape descriptors of Table II. We will denote these with a superscript, e.g., ${}^{\text{ref}}\rho_b$ for the value of the charge density at the bond critical point for the reference state of some bcc metal. These reference quantities will differ from metal to metal. However, the quantities

$$\frac{{}^{\text{ref}}\phi_r}{{}^{\text{ref}}\rho_r^{\text{ref}}\rho_b^{\text{ref}}\theta_b}, \quad \frac{{}^{\text{ref}}\phi_c}{{}^{\text{ref}}\rho_c^{\text{ref}}\rho_r^{\text{ref}}\phi_r}, \quad \text{and} \quad \frac{{}^{\text{ref}}\theta_c}{{}^{\text{ref}}\rho_c^{\text{ref}}\rho_b^{\text{ref}}\theta_b}$$

are less variable and are taken to be the constants of Eqs. (5)–(7), i.e., κ_{rb}, κ_{cr}, and κ_{cb} respectively. Obviously, this identification guarantees that the intercritical point spring constants vanish for a system in its reference state.

That κ_{cp1cp2} are nearly constants is supported by a simple model that assumes the tails of the overlapping spherical charge densities go as $e^{-\alpha r}$. It is then an easy matter to calculate the values of the reference quantities as functions of α. While the reference quantities vary with α, κ_{cp1cp2} vary more slowly and will be practically constant for a series of metals in which the tails of the reference state charge densities do not differ markedly. The compelling conclusion is that the intercritical point spring constants provide information about the amount of charge that flows from a CP in its reference state to yield the same CP in the observed state. This conclusion is entirely consistent with the interpretation of the elastic constants afforded by Eq. (4).

Unfortunately, without an exact form for the reference state there is insufficient information to calculate κ_{cr}, κ_{cb}, and κ_{rb} individually. Still, one can extract an average κ and approximate the values of the intercritical point spring constants for each of the five bcc metals. These are provided in Table III.

V. CONCLUSIONS

The GBM, even at this early stage, provides both a quantitative and simple visual representation for the stiffness of an intercritical point connection, and by extension, the values of the Cauchy pressure in bcc metals. However, there is much more that needs to be done. First, a formal method to determine the shape of the reference state is needed. One approach may be to use the methodology of Hirshfeld,[34] which has been shown to produce a reference state in which the information lost is minimized as this state evolves to

produce the observed molecular or solid state density.[35,36] Second, the picture presented here is applicable to metals with the simplest of topologies—the bcc metals. As our next step, we will address fcc metals where there are two symmetry unique irreducible bundles, four nonnuclear CPs, two of which are characterized by three distinct principal curvatures. In all, there will be 14 charge density shape descriptors. We expect that in fcc metals, in addition to the structures identified here, there will be other charge density features that play a role in mediating elastic response.

ACKNOWLEDGMENTS

We gratefully acknowledge support of this work under ONR Grant No. N00014-10-1-0838 and under ARO Grant No. 421-20-18.

*meberhar@mines.edu

[1] R. F. W. Bader, *Atoms in Molecules. A Quantum Theory* (Clarendon Press, Oxford, UK, 1990).
[2] M. Eberhart, Philos. Mag. B **81**, 721 (2001).
[3] T. Jones and M. Eberhart, Int. J. Quantum Chem. **110**, 1500 (2010).
[4] T. E. Jones and M. E. Eberhart, J. Chem. Phys. **130**, 204108 (2009).
[5] M. Blackman, Proc. R. Soc. London A **164**, 62 (1938).
[6] D. Pettifore, Mater. Sci. Technol. **8**, 345 (1992).
[7] J. Plummer and I. Todd, Appl. Phys. Lett. **98**, 021907 (2011).
[8] C. F. Matta and R. J. Boyd, eds., *The Quantum Theory of Atoms in Molecules: From Solid State to DNA and Drug Design* (Wiley-VCH Verlag GmbH & Co. KGaA: Weinheim, 2007).
[9] R. F. W. Bader, Phys. Rev. B **49**, 13348 (1994).
[10] S. Srebrenik, R. F. W. Bader, and T. T. Nguyen-Dang, J. Chem. Phys. **68**, 3667 (1978).
[11] A. Martín Pendás, M. A. Blanco, and E. Francisco, Chem. Phys. Lett. **417**, 16 (2006).
[12] P. Nasertayoob and S. Shahbazian, Int. J. Quantum Chem. **109**, 726 (2009).
[13] F. Heidarzadeh and S. Shahbazian, Int. J. Quantum Chem. **111**, 2788 (2011).
[14] P. F. Zou and R. F. W. Bader, Acta Crystallogr. Sect. A **50**, 714 (1994).
[15] A. M. Pendás, A. Costales, and V. Luaña, Phys. Rev. B **55**, 4275 (1997).
[16] T. E. Jones, M. E. Eberhart, S. Imlay, and C. Mackey, J. Phys. Chem. A **115**, 12582 (2011).
[17] T. E. Jones, J. Phys. Chem. A **116**, 4233 (2012).
[18] D. Eberly, R. Gardner, B. Morse, S. Pizer, and C. Scharlach, J. Math. Imaging Vis. **4**, 353 (1994).
[19] P. W. Ayers and S. Jenkins, J. Chem. Phys. **130**, 154104 (2009).
[20] A. Guevara-Garcia, E. Echegaray, A. Toro-Labbe, S. Jenkins, S. R. Kirk, and P. W. Ayers, J. Chem. Phys. **134**, 234106 (2011).
[21] G. Kresse and J. Furthmuller, Comput. Mater. Sci. **6**, 15 (1996).
[22] G. Kresse and J. Furthmuller, Phys. Rev. B **54**, 11169 (1996).
[23] G. Kresse and D. Joubert, Phys. Rev. B **59**, 1758 (1999).
[24] J. P. Perdew, K. Burke, and M. Ernzerhof, Phys. Rev. Lett. **77**, 3865 (1996).
[25] J. P. Perdew, J. A. Chevary, S. H. Vosko, K. A. Jackson, M. R. Pederson, D. J. Singh, and C. Fiolhais, Phys. Rev. B **46**, 6671 (1992).
[26] S. H. Vosko, L. Wilk, and M. Nusair, Can. J. Phys. **58**, 1200 (1980).
[27] TECPLOT, http://www.tecplot.com/ (2012).
[28] R. Feynman, *The Feynman Lectures on Physics* (Addison-Wesley, Boston, 1963), Vol. 2, Chap. 39, pp. 10–13.
[29] R. A. Johnson, Phys. Rev. B **37**, 3924 (1988).
[30] P. Hohenberg and W. Kohn, Phys. Rev. **136**, B864 (1964).
[31] M. Eberhart, Acta Mater. **44**, 2495 (1996).
[32] J. F. Nye, *Physical Properties of Crystals: Their Representation by Tensors and Matrices* (Oxford University Press, USA, 1985).
[33] M. E. Eberhart and A. F. Giamei, Mater. Sci. Eng. A **248**, 287 (1998).
[34] F. Hirshfeld, Theor. Chem. Acc. **44**, 129 (1977).
[35] R. F. Nalewajski and R. G. Parr, PNAS **97**, 8879 (2000).
[36] R. G. Parr, P. W. Ayers, and R. F. Nalewajski, J. Phys. Chem. A **109** (2005).